Research Article

Quantum Oscillations and Chiral Anomaly in a $Bi_{0.96}Sb_{0.04}$ Single Crystal

Gongqin Xu,[1] Anne de Visser,[2] Yingkai Huang,[2] and Xingyu Mao [1]

[1] *Jimei University, Xiamen, China*
[2] *Van der Waals-Zeeman Institute, University of Amsterdam, Science Park 904, 1098 XH Amsterdam, Netherlands*

Correspondence should be addressed to Xingyu Mao; maoxingyu@jmu.edu.cn

$Bi_{1-x}Sb_x$ alloys are of special significance in topological insulator research. Here we focus on the $Bi_{0.96}Sb_{0.04}$ alloy in which the conduction band edge just touches the valence band edge. Transport measurements show quantum oscillations in the longitudinal (Shubnikov–de Haas effect) and transverse magnetoresistance originating from a spheroidal Fermi surface pocket. Further investigation of the longitudinal magnetoresistance for the magnetic field parallel to the electrical current shows a small nonmonotonic magnetoresistance that is attributed to a competition of weak-antilocalization effects and a topological term related to the chiral anomaly.

1. Introduction

Being the first experimentally confirmed 3D topological insulator [1, 2], $Bi_{1-x}Sb_x$ alloys have attracted much attention in the past decade. The band structure of $Bi_{1-x}Sb_x$ alloys shows that when the Sb concentration is within the range $x = 0.07\text{-}0.22$, there is a gap between the inverted L_a band and L_s band. The inverted band structure results in an insulating bulk and conducting surface states, with a Dirac cone energy dispersion preserved by a nontrivial topological quantum number [3–5]. The alloy's physical properties are very sensitive to the percentage of Sb, and the evolution of the band structure and topological properties are studied over a wide Sb concentration range [6]. A special point of interest is $x = 0.04$, where the valence band and conduction band just touch each other forming a Dirac cone. Hence, $Bi_{0.96}Sb_{0.04}$ may show properties originating from Dirac fermions.

Research on 3D Dirac semimetals was spurred by the investigation of 2D Dirac fermions in graphene and has been reported frequently in the past decade [7–9]. Furthermore, the 3D Weyl semimetal has come into sight in the last couple of years [10–12], though Weyl fermions had been predicted a long time ago. Weyl semimetals that comprise Weyl fermions, which are widely studied in the context of elementary particles in high energy physics, are a new laboratory tool to study electronic nontrivial states in condensed matter systems. Weyl semimetals (WSM) are novel topological phases of 3D materials that are characterized by a set of linear-dispersive band-touching points, called Weyl nodes, which are enclosed by the Fermi surface. The Weyl nodes are stable to arbitrary perturbations, as long as charge conservation and translational invariance are preserved. Basic theoretical deduction shows that the Weyl nodes must appear in pairs with different chirality. A Weyl node acts like a magnetic monopole in momentum space [13]. In 3D systems, any perturbation with translational symmetry cannot open a gap; therefore the Weyl fermion system is topologically stable. Weyl fermions may be experimentally detected through the chiral anomaly, as proposed by Adler [14] and Bell and Jackiw [15] in 1969. The chiral anomaly is the anomalous nonconservation of a chiral current. In 1983 it was pointed out that this may result in a high conductivity when the magnetic field is applied along the electric current [16]. A theoretical explanation is offered by Weyl nodes with opposite chirality and separated in momentum space and in energy, giving rise to an induced topological θ-term in the action of the electromagnetic field [17, 18]

$$S_\theta = \frac{e^2}{8\pi^2} \int dt d\boldsymbol{r} \theta(\boldsymbol{r}, t) \, \boldsymbol{E} \cdot \boldsymbol{B}. \tag{1}$$

Here $\hbar = c = 1$ and $\theta(\boldsymbol{r},t)=2(\boldsymbol{b} \cdot \boldsymbol{r} - b_0 t)$, where b denotes the shift in energy. Recently, it was proposed that the chiral anomaly resulting from the $\boldsymbol{E} \cdot \boldsymbol{B}$ term may be verified in a magnetoresistance experiment, by applying the magnetic field parallel to the electric current, which should lead to a large negative magnetoresistance. This could be regarded as a fingerprint of a Weyl semimetal [11, 19].

Here we report a magnetotransport study taken on a single crystalline $Bi_{1-x}Sb_x$ alloy at the Weyl point composition $Bi_{0.96}Sb_{0.04}$. We have investigated the electronic structure at the Fermi surface via magnetoresistance and quantum oscillations and report the effect of the chiral anomaly.

2. Experimental Details

A single crystal (SC) $Bi_{0.96}Sb_{0.04}$ is synthesized using a modified Bridgman method in a cone-shaped quartz tube with starting materials high purity Bi (5N) and Sb (6N). The transport properties were measured using a standard six-point contact configuration in a Physical Property Measurement System (PPMS) of Quantum Design, in applied magnetic fields up to 9 T. The size of the magnetotransport crystal is length×width×thickness = 6.1×2.8×1.5 mm^3, and the voltage and current contacts were made on the cleaved (111) plane. The crystal was mounted on a horizontal rotation stage, which allowed to vary the angle between the magnetic field and sample surface. Different crystals taken from the same $Bi_{0.96}Sb_{0.04}$ batch showed overall a very good consistency in the measured transport properties.

3. Basic Transport Properties

The basic transport properties of SC $Bi_{0.96}Sb_{0.04}$ are shown in Figure 1. The resistance measured in the temperature range 2-300 K is semiconducting-like down to 120 K and then becomes metallic-like at lower temperatures, as shown in panel (a). The longitudinal resistance R_{xx} (MR) and transverse or Hall resistance R_{xy} (HR) were measured in magnetic fields up to 9 T at several temperatures. The data were (anti)symmetrized by measuring R_{xx} and R_{xy} for both polarities of the magnetic field, thus compensating for the possible misalignment of the voltage contacts. The magnetoresistance is reported in Figure 1(b). The curves show that the MR bears many characteristic features, such as the weak-antilocalization effect (WAL) at low magnetic field, large and nonsaturated linear magnetoresistance in the high field range, and quantum oscillations below 20 K. These are all hot topics in the research on topological materials nowadays [20–22]. The carrier density and the mobility of the crystal derived after symmetrizing the data are shown in Figure 1(c). The charge carriers change from hole type to electron type as the temperature is increased to above 200 K. The carrier mobility is as high as 1.7 m^2/Vs at 2 K and exhibits a gradual decrease with increasing the temperature. This behavior is similar to that observed in conventional semimetals and semiconductors.

Next we discuss the Shubnikov–de Haas (SdH) effect. By subtracting a smooth polynomial function as background of the MR(B)-curves in Figure 1(b), we obtain the oscillatory

part of the magnetoresistance (δMR). δMR is plotted in Figure 2(a) against the inverse of the magnetic field and its periodic nature shows it is a SdH oscillation. The Fast Fourier Transform (FFT) gives a frequency $f = 20 \pm 2$ T. Besides the SdH effect in R_{xx}, we also observed quantum oscillations in R_{xy} (raw data not shown); see Figure 2(b). A FFT of δHR shows the same frequency as in R_{xx} within the experimental error. Since we have properly symmetrized the data, the oscillation in δHR is a genuine effect, which is furthermore demonstrated by the fact that the oscillations in δMR and δHR are in antiphase [23]. The observation of quantum oscillations in the Hall resistance in Bi compounds is not uncommon [24].

We analyzed the amplitude of the quantum oscillations, $\delta R/R$, by fitting the data with the Lifshitz–Kosevich theory [25].

$$\frac{\delta R}{R} \propto \sqrt{B} \exp\left(-\frac{\alpha T_D m^*}{B}\right) \frac{\alpha T m^*/B}{\sinh\left(\alpha T m^*/B\right)} \qquad (2)$$

Here T_D is the Dingle temperature, m^* is the effective mass, and $\alpha = 2\pi^2 k_B/\hbar e$. The fitting results are shown in Figure 3.

The derived effective carrier mass m^* is 0.10-0.11m_e, while the Dingle temperature falls in the range 0.96-1.97 K, with an averaged value 1.38 K. From the Dingle temperature another important parameter can be obtained, namely, the quantum lifetime τ_D, since $T_D = \hbar/2\pi k_B \tau_D$. We estimate $\tau_D = 8.81 \times 10^{-13}$ s, which results in a mobility $\mu = 15186$ cm^2/Vs. This value is consistent with the one we calculated from the Hall effect shown in Figure 1(c).

Since the $Bi_{1-x}Sb_x$ alloy, for a certain range of x-values, could be a topological insulator, the electronic transport of the sample may be due to surface Dirac electrons [26]. To investigate this the angular variation of the magnetoresistance has been measured. Figure 4(a) shows the field dependence of the MR at various angles, where θ is the angle between the magnetic field and the sample surface. The experiment was realized by tilting the sample holder gradually in the magnetic field as shown in the schematic drawing in Figure 4(a). It is important to notice that the direction of the magnetic field B is always kept perpendicular to the electrical current I, while tuning the angle θ.

After subtracting the background we obtained the SdH signal, which is plotted in Figure 4(b) as a function of $1/(B\cos\theta)$. The period evolves with $1/(B\cos\theta)$, which shows that the SdH signal does not originate from surface states with a 2D Fermi surface. In Figure 4(c) the frequencies are plotted as a function of θ. Here we also compare the data with the theoretical curves for a cylindrical Fermi surface (blue line) and a bulk spheroidal Fermi surface (red line). A reasonable agreement can be obtained by assuming a spheroidal hole pocket with a major half axis of 5.6×10^8 m^{-1} and minor half axis of 2.5×10^8 m^{-1}.

4. Chiral Anomaly

Next we rotate the magnetic field from 'parallel to' the current I to 'perpendicular to' the current and sample surface, which
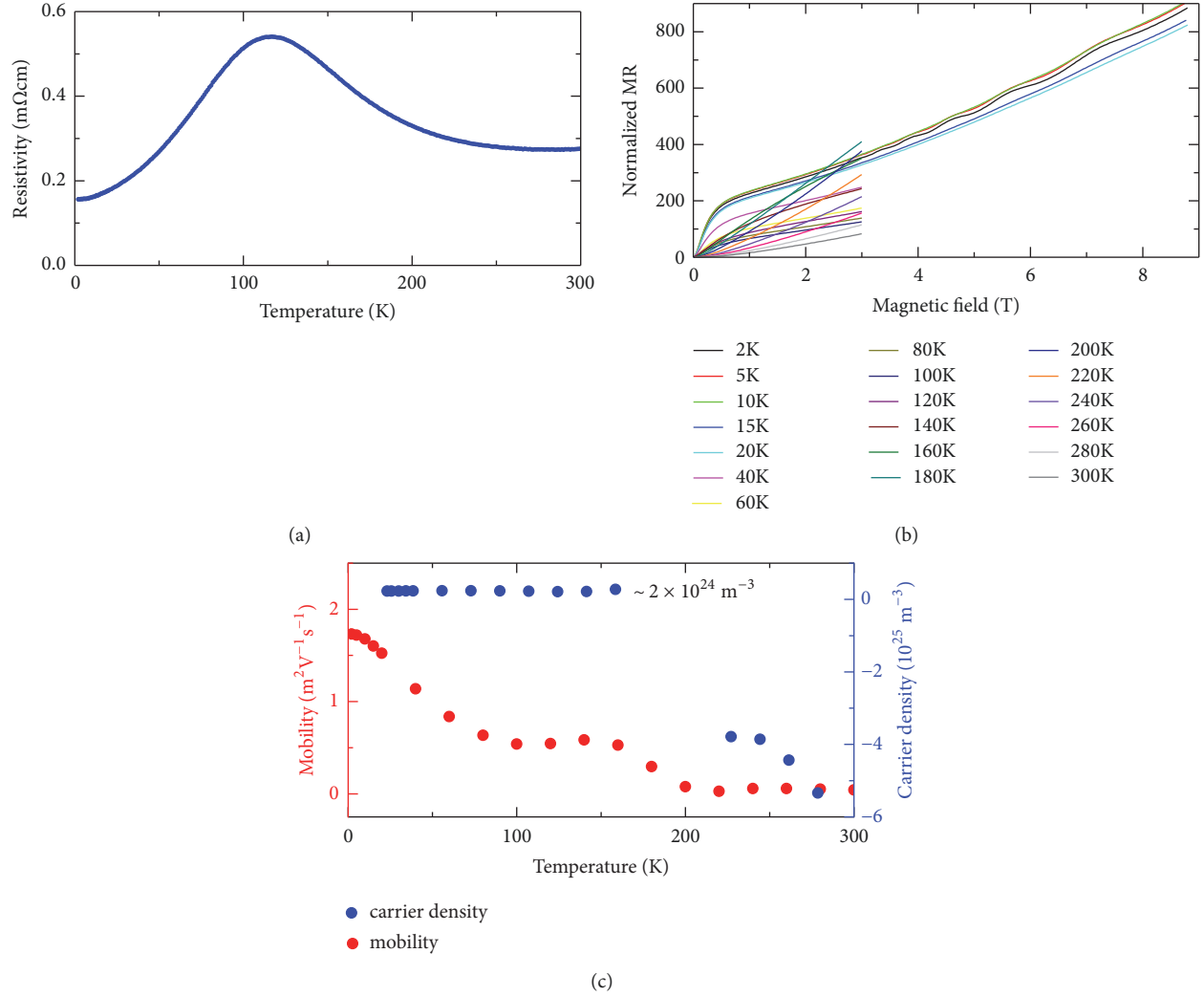
FIGURE 1: Transport properties of $Bi_{0.96}Sb_{0.04}$. (a) Resistivity in zero magnetic field. (b) Magnetoresistance at various temperatures. Quantum oscillations are visible at temperatures of 2, 5, 10, and 15 K. (c) Mobility (red symbols) and carrier density (blue symbols) at different temperatures. In the temperature range 180-220 K we could not extract a reliable value of the carrier density.

reveals another interesting behavior. Selected magnetoresistance curves obtained at a temperature of 2 K for $75° < \theta < 105°$ are shown in Figure 5. Here θ is the rotation angle of the magnetic field with $\theta = 0$ for $B \perp I$ and $\theta = 90°$ for B $\parallel$ I; see the schematic drawing in Figure 5. When the magnetic field is close to 'parallel to' the current we observe a number of features. At very low fields the positive magnetoresistance is due to WAL, but then an oscillatory behavior sets in with a local maximum around 1 T and a deep minimum around 1.5 T. The oscillatory behavior is systematic for a field tilt up to ±5° with respect to the current and extends up to 9 T. Obviously it is not a SdH oscillation which is periodic in $1/B$. The small magnetoresistance for $B \parallel I$ is most likely associated with the chiral anomaly. The modest MR values seem to result from the competition between the negative magnetoresistance and the strong WAL. This effect is only observed for field angles close to the current. For larger tilt

angles, e.g., $\theta = 75°$, $100°$, and $105°$, the MR is large and positive. Similar features in the MR of $Bi_{0.97}Sb_{0.03}$ have been reported by Kim et al. [19, 27]. These authors analyzed the conductivity data with a simple model with Drude, WAL, and topological ($E \cdot B$ term) contributions and also concluded that the (negative) MR could be the result of the competition between WAL and the chiral anomaly term. We remark that the magnetoresistance of pure Bi does not show the anomalous behavior related to the chiral anomaly as shown in the inset of Figure 5. Recently, Gorba et al. [28] have evaluated the magnetoconductivity tensor of Dirac and Weyl semimetals with the Kubo's linear response theory and also found an oscillatory behavior in magnetic field, but here it is related to the SdH effect. It is still a challenging task to solve the negative MR theoretically as a consequence of the chiral anomaly.
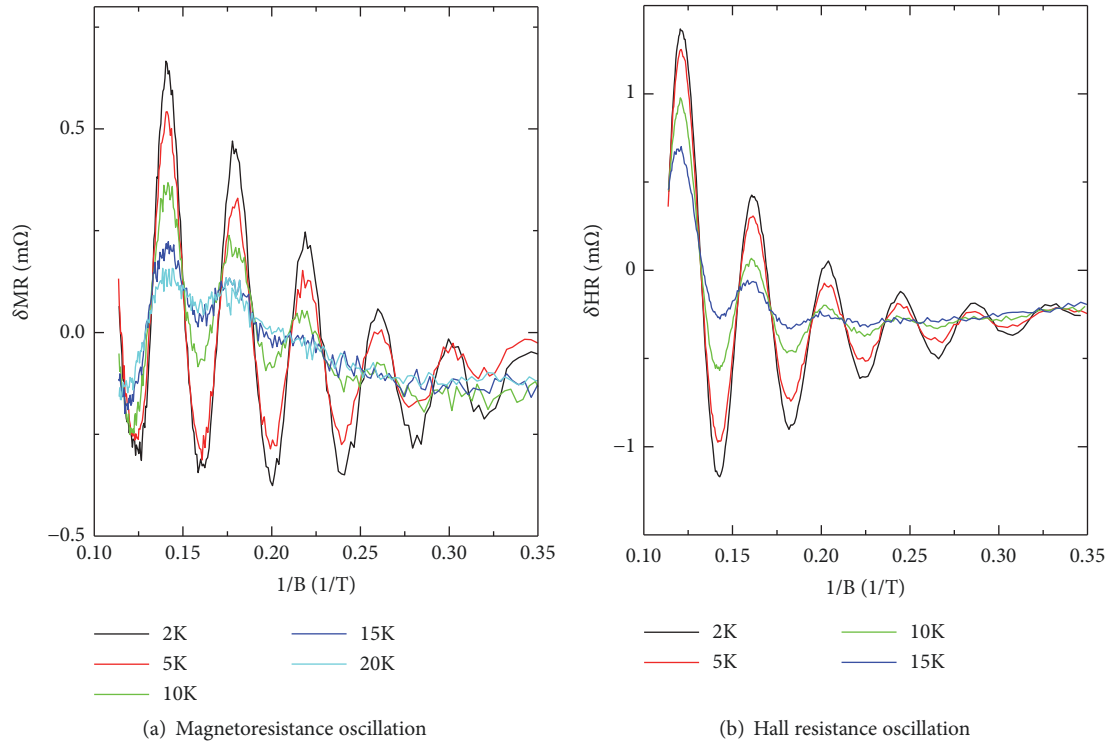
(a) Magnetoresistance oscillation

(b) Hall resistance oscillation

FIGURE 2: Quantum oscillations in $Bi_{0.96}Sb_{0.04}$ (a) in the longitudinal magnetoresistance MR and (b) in the Hall resistance HR. Note that the oscillations in MR and HR are in antiphase.
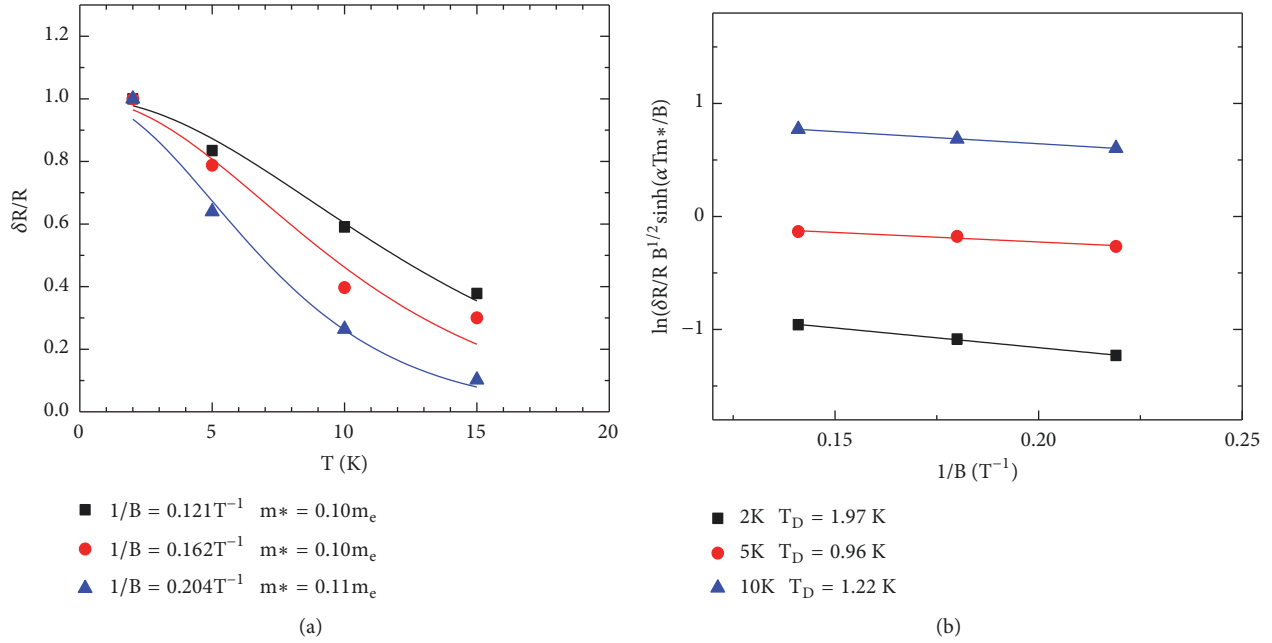

(a)

(b)

FIGURE 3: Results of fitting the SdH oscillations in the MR with the Lifshitz–Kosevich theory. (a) Temperature dependence of the SdH oscillation amplitude $\delta R/R$ at $B = 8.26$ T, 6.17 T, and 4.9 T. (b) Dingle plot at $T = 2$ K, 5 K, and 10 K.
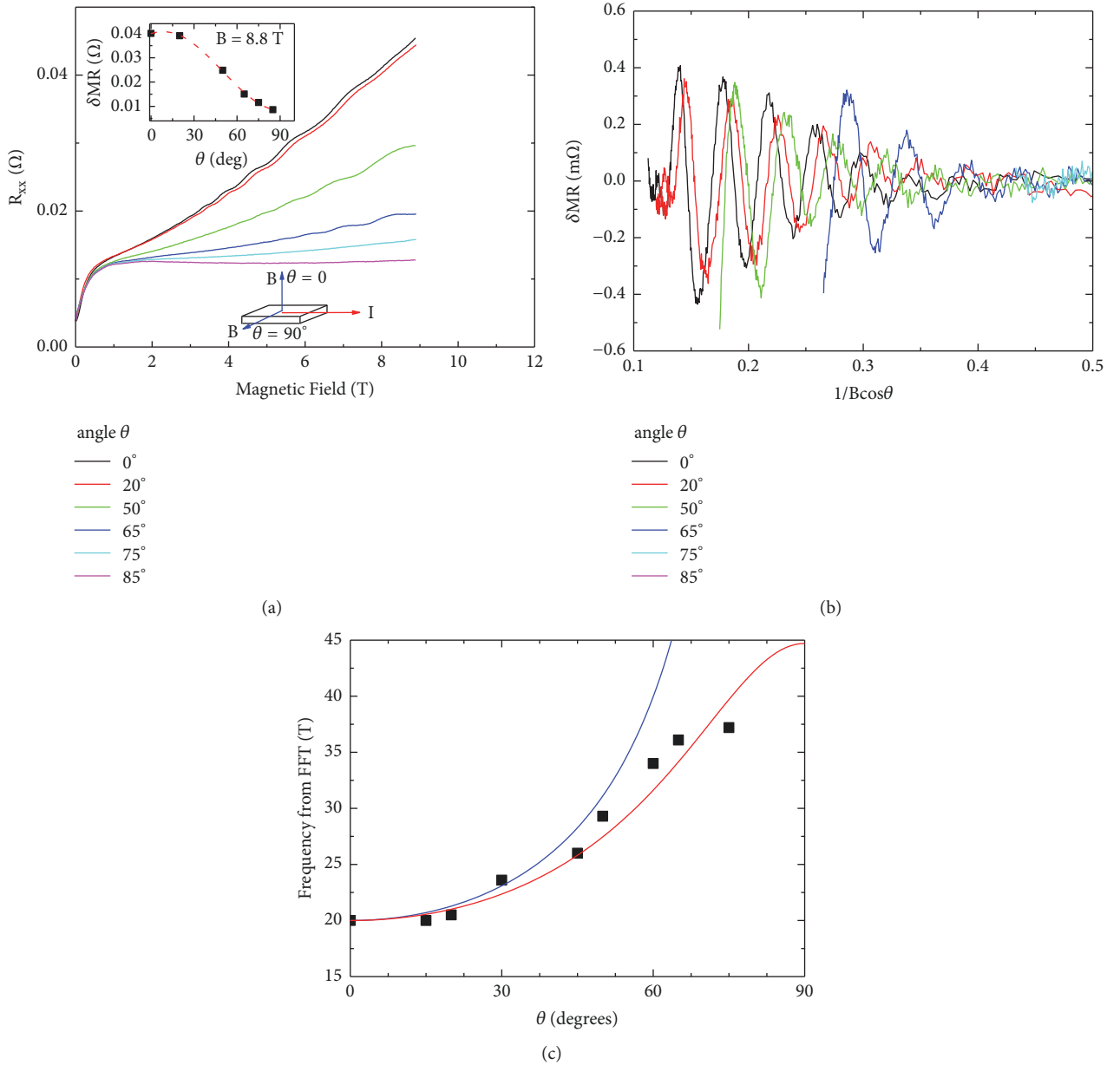
FIGURE 4: (a) Magnetoresistance at different angles, where θ is the angle between the magnetic field and the sample surface. The data are taken at $T = 2$ K. Inset: variation of the MR in a magnetic field of 8.8 T. (b) SdH oscillations at various angles plotted against $1/(B\cos\theta)$. (c) Angular variation of the SdH frequencies obtained by FFT. Symbols: data points; blue line: expected behavior for a cylindrical Fermi surface; red line: comparison with a spheroidal Fermi surface.

5. Summary

In summary, we have studied the magnetotransport properties of a $Bi_{1-x}Sb_x$ single crystal with $x = 0.04$, *i.e.*, the concentration for which a Dirac point is expected in the bulk band structure. SdH oscillations are found in the longitudinal and transverse magnetoresistance with $f = 20\pm2$ T. These are attributed to a 3D spheroidal Fermi surface. Magnetoresistance experiments for the field along the current direction show a small magnetoresistance with unusual oscillatory behavior. This is attributed to a competition between WAL and the effect of the chiral anomaly due to Weyl points.

Data Availability

The data used to support the findings of this study are available from the corresponding author upon request.

Conflicts of Interest

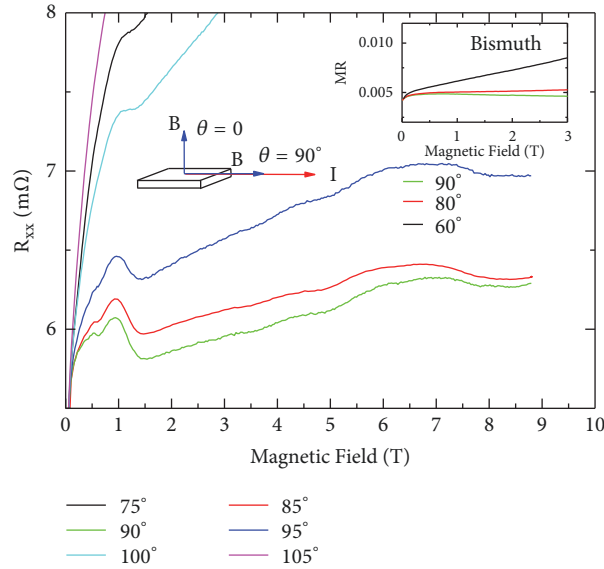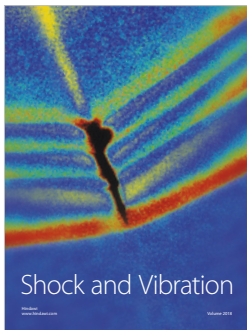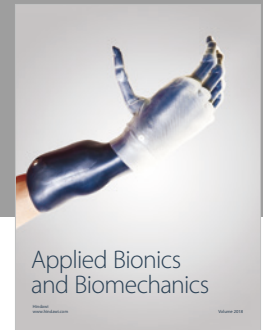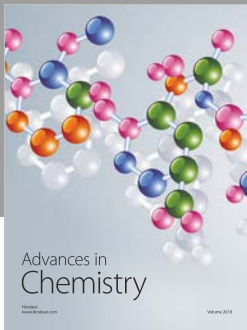The authors declare that they have no conflicts of interest.

Acknowledgments

FIGURE 5: Magnetoresistance measured for different angles between the magnetic field B and the current I, as indicated in the schematic drawing. At $\theta = 90^o$ $B \parallel I$. The data are taken at $T = 2$ K. The inset shows the magnetoresistance of a pure Bi single crystal for 3 different angles θ.

References

[1] L. Fu and C. L. Kane, "Topological insulators with inversion symmetry," *Physical Review B*, vol. 76, Article ID 045302, 2007.

[2] D. Hsieh, D. Qian, L. Wray et al., "A topological dirac insulator in a quantum spin hall phase," *Nature*, vol. 452, pp. 970–974, 2008.

[3] M. Z. Hasan and C. L. Kane, "Colloquium: topological insulators," *Reviews of Modern Physics*, vol. 82, pp. 3045–3067, 2010.

[4] J. E. Moore, "The birth of topological insulators," *Nature*, vol. 464, pp. 194–198, 2010.

[5] C. L. Kane and E. J. Mele, "Z_2 topological order and the quantum spin hall effect," *Physical Review Letters*, vol. 95, Article ID 146802, 2005.

[6] F. Nakamura, Y. Kousa, A. Taskin et al., "Topological transition in $Bi_{1-x}Sb_x$ studied as a function of Sb doping," *Physical Review B*, vol. 84, Article ID 235308, 2011.

[7] S. M. Young, S. Zaheer, J. C. Y. Teo et al., "Dirac semimetal in three dimensions," *Physical Review Letters*, vol. 108, Article ID 140405, 2012.

[8] Z. Wang, H. Weng, Q. Wu, X. Dai, and Z. Fang, "Three-dimensional Dirac semimetal and quantum transport in Cd_3As_2," *Physical Review B*, vol. 88, Article ID 125427, 2013.

[9] S. Borisenko, Q. Gibson, D. Evtushinsky, V. Zabolotnyy, B. Büchner, and R. J. Cava, "Experimental realization of a three-dimensional dirac semimetal," *Physical Review Letters*, vol. 113, Article ID 027603, 2014.

[10] K. Y. Yang, Y. M. Lu, and Y. Ran, "Quantum hall effects in a weyl semimetal: possible application in pyrochlore iridates," *Physical Review B*, vol. 84, Article ID 075129, 2011.

[11] P. Hosur and X. Qi, "Recent developments in transport phenomena in Weyl semimetals," *Comptes Rendus Physique*, vol. 14, pp. 857–870, 2013.

[12] G. B. Halász and L. Balents, "Time-reversal invariant realization of the Weyl semimetal phase," *Physical Review B*, vol. 85, Article ID 035103, 2012.

[13] H. Weng, C. Fang, Z. Fang, B. A. Bernevig, and X. Dai, "Weyl semimetal phase in noncentrosymmetric transition-metal monophosphides," *Physical Review X*, vol. 5, Article ID 011029, 2015.

[14] S. L. Adler, "Axial-vector vertex in spinor electrodynamics," *Physical Review*, vol. 177, Article ID 2426, 1969.

[15] J. S. Bell and R. Jackiw, "A PCAC puzzle: $\pi^0 \longrightarrow \gamma\gamma$ in the σ-model," *Il Nuovo Cimento A*, vol. 60, pp. 47–61, 1969.

[16] H. B. Nielsen and M. Ninomiya, "The Adler-Bell-Jackiw anomaly and Weyl fermions in a crystal," *Physics Letter B*, vol. 130, pp. 389–396, 1983.

[17] M. M. Vazifeh and M. Franz, "Self-organized topological state with majorana fermions," *Physical Review Letters*, vol. 111, Article ID 206802, 2013.

[18] A. A. Zyuzin and A. A. Burkov, "Weyl semimetal with broken time reversal and inversion symmetries," *Physical Review B*, vol. 85, Article ID 165110, 2012.

[19] H. J. Kim, K. S. Kim, J. F. Wang et al., "Dirac versus weyl fermions in topological insulators: adler-bell-jackiw anomaly in transport phenomena," *Physical Review Letters*, vol. 111, Article ID 246603, 2013.

[20] H. T. He, G. Wang, T. Zhang et al., "Impurity effect on weak antilocalization in the topological insulator Bi_2Te_3," *Physical Review Letters*, vol. 106, Article ID 166805, 2011.

[21] M. Novak, S. Sasaki, K. Segawa, and Y. Ando, "Large linear magnetoresistance in the dirac semimetal TlBiSSe," *Physical Review B*, vol. 91, Article ID 041203, 2015.

[22] K. Shrestha, V. Marinova, B. Lorenz, and P. C. W. Chu, "Shubnikov–de Haas oscillations from topological surface states

of metallic $Bi_2Se_{2.1}Te_{0.9}$," *Physical Review B*, vol. 90, Article ID 241111, 2014.

[23] A. Ishihara and L. Smrcka, "Density and magnetic field dependences of the conductivity of two-dimensional electron systems," *Journal of Physics C*, vol. 19, pp. 6777–6789, 1986.

[24] J. M. Reynolds, H. W. Hemstreet, T. E. Leinhardt, and D. D. Triantos, "Hall effect in bismuth at low temperatures," *Physical Review*, vol. 96, Article ID 1203, 1954.

[25] D. Shoenberg, Magnetic oscillations in metals, Cambridge University Press, Cambridge, UK, 1984.

[26] Y. Yan, L. X. Wang, D. P. Yu, and Z. M. Liao, "Large magnetoresistance in high mobility topological insulator Bi_2Se_3," *Applied Physics Letters*, vol. 103, Article ID 033106, 2013.

[27] K. S. Kim, H. J. Kim, M. Sasaki, J. F. Wang, and L. Li, "Anomalous transport phenomena in Weyl metal beyond the Drude model for Landau's Fermi liquids," *Science and Technology of Advanced Materials*, vol. 15, Article ID 064401, 2014.

[28] E. V. Gorbar, V. A. Miransky, and I. A. Shovkovy, "Chiral anomaly, dimensional reduction, and magnetoresistivity of weyl and dirac semimetals," *Physical Review B*, vol. 89, Article ID 085126, 2014.

Advances in
Chemistry

Journal of
Engineering

The Scientific
World Journal

International Journal of
Geophysics

Applied Bionics
and Biomechanics

Shock and Vibration

Active and Passive
Electronic Components

Advances in
Mathematical Physics

Hindawi

Submit your manuscripts at
www.hindawi.com

Advances in
Astronomy

Advances in
OptoElectronics

International Journal of
Rotating
Machinery

Advances in
Physical Chemistry

Advances in
Condensed Matter Physics

Advances in
Optical
Technologies

Journal of
Chemistry

International Journal of
Antennas and
Propagation

Advances in
High Energy Physics

Advances in
Acoustics and Vibration

International Journal of
Optics